Published in final edited form as:
Biomaterials. 2012 October ; 33(29): 7174–7181. doi:10.1016/j.biomaterials.2012.06.024.

Anti-CD20 multivalent HPMA copolymer-Fab′ conjugates for the direct induction of apoptosis

Te-Wei Chu[a], **Jiyuan Yang**[a], and **Jindřich Kopeček**[a,b,*]

[a]Department of Pharmaceutics and Pharmaceutical Chemistry, University of Utah, Salt Lake City, Utah 84112, USA

[b]Department of Bioengineering, University of Utah, Salt Lake City, Utah 84112, USA

Abstract

A hybrid biomimetic system comprising high-molecular-weight, linear copolymer of *N*-(2-hydroxypropyl)methacrylamide (HPMA) grafted with multiple Fab′ fragments of anti-CD20 monoclonal antibody (mAb) was synthesized by reversible addition-fragmentation chain transfer (RAFT) polymerization followed by attachment of Fab′ fragments via thioether bonds. Exposure of human non-Hodgkin's lymphoma (NHL) Raji B cells to the multivalent conjugates resulted in crosslinking of CD20 receptors and commencement of apoptosis. Five conjugates with varying molecular weight and valence (amount of Fab′ per polymer chain) were synthesized. One of the copolymers contained enzyme degradable peptide sequences (GFLG) in the backbone. The multivalency led to higher avidity and apoptosis induction compared to unconjugated whole mAb. Time-dependent studies showed that the cytotoxicity of conjugates exhibited a slower onset at shorter exposure times than mAb hyper-crosslinked with a secondary Ab; however, at longer time intervals the HPMA copolymer conjugates achieved significantly higher biological efficacies. In addition, study of the relationship between the structure of conjugates and Raji B cell apoptosis revealed that both valency and polymer molecular weight influenced biological activities, while insertion of peptide sequences into the backbone was not a factor *in vitro*.

Keywords

HPMA; CD20; Non-Hodgkin's lymphoma; Rituximab; B cell; Multivalency

1. Introduction

The use of hybrid biomaterials composed of synthetic and biological macromolecules to design "smart" nanomedicines is an emerging field [1,2]. The goals include precise targeting to diseased sites, enhancing therapeutic efficiency, reducing adverse effects, and minimizing drug resistance. In particular, water-soluble HPMA copolymers are extensively used as delivery vehicles to conjugate anticancer therapeutic agents (*e.g.* small molecule drugs) and targeting moieties (*e.g.* antibodies) [3]. HPMA polymer and copolymers have favorable physicochemical and pharmacokinetic properties to provide a well-defined safety profile, increase circulation half-life of therapeutics, and provide a flexible (random coil) conformation of the polymer backbone in solution [4]. The design of macromolecular therapeutics has extended towards a unique paradigm where biomimetic strategies are used

*Corresponding author. University of Utah, Center for Controlled Chemical Delivery, 2030 East 20 South, Biopolymers Research Building, Room 205B, Salt Lake City, Utah 84112-9452, USA. Tel.: +1 (801) 581 7211; fax: +1 (801) 581 7848. jindrich.kopecek@utah.edu (J. Kopeček).

to trigger specific responses or facilitate therapeutic efficiency through innate biological processes [1,3,5,6]. For instance, an HPMA-based hybrid system has been used as a "drug-free" macromolecular platform to induce apoptosis via biorecognition and receptor crosslinking at the cell surface; a clinically relevant therapeutic efficacy was demonstrated *in vitro* [6] and *in vivo* [7].

Non-Hodgkin's lymphoma (NHL) is a prevalent cancer in the United States with a history of over a half-million incidences and projected 70,130 new cases diagnosed in 2012 [8]. Because about 85% of NHL is of B cell origin and more than 95% of B lymphomas bear the CD20 surface antigen [9], immunotherapies using anti-CD20 monoclonal antibodies (mAb) have revolutionized the treatment of NHL [10]. However, the overall response levels to clinically used mAb, mainly rituximab (Rituxan®), for treatments of relapsed/refractory low-grade or follicular NHLs are less than 50% [11]. Rare but lethal side effects such as progressive multifocal leukoencephalopathy (PML) and lung injuries observed in patients treated with rituximab or other anti-CD20 mAb also raised biocompatibility concerns [12–15]. Therefore, new therapeutic strategies are needed.

The clinical non-responsiveness and adverse effects of rituximab or other therapeutic mAb has been partly attributed to the Fc fragment-related biological events [14,16–18]. The inactivity of effector cells to hyper-crosslink bound rituximab on B cell surface via Fc results in failure of antibody-dependent cellular cytotoxicity (ADCC) and complement-dependent cytotoxicity (CDC), the main thrusts of anti-CD20 mAb's therapeutic effect [16,18–20]. In addition, Fc-mediated cellular events such as complement activation or the surge release of tumor necrosis factor-α (TNFα) upon mAb infusion are related to the severe side effects [12,14,17]. Consequently, approaches aiming at direct apoptosis induction through cell surface receptor clustering are becoming attractive [21–25]. In these previous studies, either multimeric Abs covalently linked to each other [24,25], bound to dextran [22], to lipid nanoparticles [23], or monomeric Ab lacking effector cell functions hyper-crosslinked by a secondary Ab [21] were used to specifically enhance apoptosis. In particular, Rossi *et al.* developed a hexavalent anti-CD20 Ab by covalently assembling 6 Fab′ to 1 Fc, and demonstrated that its anti-tumor efficacy in murine model was comparable to mAb monomer (Veltuzumab), but without any sign of CDC [25].

We have reported a hybrid biomimetic system composed of branched HPMA copolymer and multiple Fab′ fragments of the anti-CD20 mAb (1F5) which targets and crosslinks CD20 on the surface of B cells [26,27]. We hypothesized that the crosslinking would lead to clustering of (non-internalizing) CD20 antigens and induction of apoptosis via CD20-mediated signaling pathways. The design features the absence of Fc fragment and multimeric interactions with targets. Superior binding affinity [26] and apoptosis induction [27] when compared to unconjugated mAb were observed in several B cell lines. Here we aimed to improving this system using high-molecular-weight linear HPMA copolymers synthesized by controlled radical polymerization. This provided tailor-made multivalent conjugates with narrow molecular weight distribution, precise control of valences (Fab′ content per polymer chain), well-defined and reproducible architectures, and potentially longer circulating half-lives. The improved design permitted the study of the relationship between the structure of conjugates and their biological activities, which facilitated the understanding of processes involved in CD20-crosslinking mediated apoptosis induction.

2. Materials & methods

2.1. Materials

N-(3-Aminopropyl)methacrylamide hydrochloride (APMA) was purchased from Polysciences (Warrington, PA). 4,4′-azobis(4-cyanopentanoic acid) (V-501) was from

Wako Chemicals (Richmond, VA). Succinimidyl-4-(*N*-maleimidomethyl)cyclo-hexane-1-carboxylate (SMCC) and sulfo-SMCC were purchased from Soltec Ventures (Beverly, MA). o-Phthalic dicarboxaldehyde (OPA) and 3-mercaptopropionic acid (MPA) were purchased from Sigma-Aldrich (St. Louis, MO). *N*-(2-Hydroxypropyl) methacrylamide (HPMA) [28] and 4-cyanopentanoic acid dithiobenzoate (CPDB) [29] were prepared as previously described. All solvents were obtained from Sigma-Aldrich as the highest purity available.

2.2. Cell line, hybridoma, and Fab′ fragment preparation

Human Burkitt's B cell non-Hodgkin's lymphoma Raji cell line (ATCC, Bethesda, MD) was used for biological evaluations. Cells were cultured in RPMI-1640 medium (Sigma, St. Louis, MO) supplemented with 10% fetal bovine serum (Hyclone, Logan, UT) and grown at 37 °C in a humidified atmosphere with 5% CO_2 (v/v). All experiments were performed using cells in exponential growth phase. Murine 1F5 anti-CD20 IgG2a antibody was prepared from the hybridoma clone 1F5 in a CellMax bioreactor (Spectrum Laboratories, Rancho Dominguez, CA) according to the manufacturer's instructions. Cells were initially cultured in aforementioned conditions and adapted to chemically defined, serum-free medium (Invitrogen, Carlsbad, CA). Anti-CD20 mAb was purified on a Protein G Sepharose 4 Fast Flow column (GE Healthcare, Piscataway, NJ) from bioreactor harvest supernatant. Preparation of Fab′ fragment from the whole Ab was achieved using a previously reported procedure [6, 26]. Briefly, 1F5 mAb was digested into F(ab′)$_2$ with 10% (w/w) pepsin (Sigma, St. Louis, MO) in 0.1 M citric buffer (pH 4.0) and labeled with Rhodamine Red™-X succinimidyl ester (R6010) (Molecular Probes®, Invitrogen). Immediately before use, 5 mg/mL of F(ab′)$_2$ was reduced to Fab′ with 5 mM tris(2-carboxyethyl)phosphine (TCEP) (Thermo Scientific, Waltham, MA) in 0.1 M phosphate buffered saline (PBS) (pH 6.5).

2.3. HPMA copolymers and polymer precursors

Synthesis of HPMA copolymer with pendent amino groups (P-NH_2) and its conversion into maleimide-derivatized polymer precursor (P-mal) are depicted in Fig. 1. P-NH_2 was synthesized by reversible addition-fragmentation chain transfer (RAFT) copolymerization of HPMA and APMA in deionized (DI) water at 70 °C using CPDB as chain transfer agent (CTA) and V-501 as initiator. For the backbone degradable polymer precursor, a bifunctional dithiobenzoate containing enzyme cleavable oligopeptide Gly-Phe-Leu-Gly (GFLG) was synthesized [29] and used as CTA (N^{α},N^{ε}-bis(4-cyano-4-(phenylcarbonothioylthio)pentanoylglycylphenylalanylleucylglycyl)lysine, abbreviated peptide2CTA) (Fig. 1A). A typical polymerization was as follows: HPMA (134.6 mg, 0.94 mmol) and APMA (10.7 mg, 0.06 mmol) were added into an ampoule attached to a Schlenkline. After three vaccum-nitrogen cycles to remove oxygen, 0.46 mL degassed DI H_2O was added to dissolve monomers, followed by addition of CPDB solution (0.35 mg in 60 μL methanol) and V-501 solution (0.12 mg in 60 μL methanol) via syringe. The mixture was bubbled with nitrogen for 15 min before sealing the ampoule; the copolymerization was performed at 70 °C for 20 h. The copolymer was isolated by precipitation into acetone and purified by dissolution-precipitation in methanol-acetone twice and dried under vacuum. Yield of P-NH_2 was 127 mg (87.3%). The molecular weight (Mw) and molecular weight distribution (Mw/Mn) were determined by size-exclusion chromatography (SEC) on ÄKTA FPLC system (GE Healthcare, Piscataway, NJ) equipped with miniDAWN and OptilabREX detectors. Superose 6 HR10/30 column (GE Healthcare) was used with sodium acetate buffer and 30% acetonitrile (v/v) (pH = 6.5) as mobile phase. The content of amino groups in the copolymer was determined by ninhydrin assay [30].

After polymerization, P-NH_2 copolymers were reacted with 2,2′-azobis(2,4-dimethyl valeronitrile) (V-65) (Wako Chemicals) to remove the terminal (active) dithiobenzoate groups. Briefly, HPMA copolymer (45 mg, Mn = 105 kDa, 0.43 μmol) and V65 (20×

excess, 2.13 mg, 8.57 μmol) were added into an ampoule. After three vacuum-nitrogen cycles to remove oxygen, 0.4 mL methanol was added. The solution was bubbled with nitrogen for 15 min, sealed and reacted at 50 °C for 3 h. The end-modified copolymer was purified by precipitation into acetone twice and then dried under vacuum (yield 42 mg).

The side chain amino groups of P-NH_2 were converted to maleimides by reaction with SMCC or sulfo-SMCC in DMF in the presence of triethylamine (TEA). A mixture of 42 mg P-NH_2 (12.6 μmol NH_2) and SMCC (12.7 mg, 37.8 μmol) was dissolved in 0.5 ml DMF followed by dropwise addition of TEA (ratio of [NH_2]:[SMCC]:[TEA] = 1:3:3), then kept at room temperature overnight. The product was precipitated into acetone/ether (2:1, v/v), filtered, and redissolved in methanol, precipitated into acetone again, filtered and dried under vacuum. The amount of maleimide in copolymer was determined by a modified Ellman's assay [31]. The conversion of amine into maleimido groups was 54%–59% with SMCC and >80% when sulfo-SMCC was used.

2.4. Preparation of multivalent conjugates

The polymer precursors P-mal were conjugated with reduced 1F5 Fab′ fragments via thioether bonds following a previously established protocol [32]. In brief, 10 mg of P-mal were dissolved in 100 μL of DMSO, and the solution was added to Fab′ (5 mg/mL) in PBS (pH 6.5) (ratio of [mal]:[Fab′] = 5:1). The products were purified on a Superose 6 HR16/60 column (GE Healthcare) to remove unbound Fab′, if any. The HPMA copolymer-Fab′ conjugates (P-Fab′) containing varying amounts of Fab′ per macromolecule were collected and analyzed on a Superose 6 HR10/30 column (Supplementary Data Fig. S1). Fab′-equivalent concentration of conjugates was determined by UV spectroscopy, measuring absorbance at 280 nm on a Varian Cary 400 Bio UV-visible spectrophotometer, and confirmed by bicinchoninic acid (BCA) protein assay (Thermo Scientific).

2.5. Determination of valences and effective diameters of P-Fab′ conjugates

A modified amino acid analysis procedure was utilized to determine the concentrations of both amino acid residues from Fab′ and 1-amino-2-propanol derived from HPMA polymer backbone. This enables the calculation of valence (number of Fab′ per polymer chain) of P-Fab′ conjugates. In practice, after hydrolysis in 6 N HCl (125 °C, 24 h), samples were pre-column derivatized with o-phthalic dicarboxaldehyde in the presence of 3-mercaptopropionic acid, and analyzed by HPLC (Agilent Technologies, Santa Clara, CA) equipped with an Eclipse XDB-C8 column and fluorescence detector (excitation 229 nm, emission 450 nm). Free 1F5 Fab′ and HPMA homopolymer were used for calibration (Supplementary Data Fig. S2).

The effective diameters of HPMA copolymer-Fab′ conjugates were analyzed by dynamic light scattering using a Brookhaven BI-200SM goniometer and BI-9000AT digital correlator equipped with a He–Ne laser (λ = 633 nm) at room temperature in PBS (pH 7.4). The scattering angle was 90°. Samples in PBS (1 mg/mL, Fab′ equivalent concentration) were filtered through a 0.45 μm filter before measurement. To rule out the possibility of aggregation of P-Fab′ conjugates in solution, samples were also measured at lower concentrations (0.5, 0.25 mg/mL) (Supplementary Data Fig. S3). P-NH_2 polymer precursors, 1F5 mAb, and Fab′ fragment were also analyzed. All measurements were performed in at least triplicate.

2.6. Confocal fluorescence microscopy

Confocal fluorescence microscopy was used to detect the biorecognition of (rhodamine-labeled) P-Fab′ conjugates at the surface of Raji B cells. Cells at a density of 2.5–5 × 10^5 per well were incubated with 0.5 mL of varying concentrations of conjugates (1, 2, 5, and 10

μM) in culture medium at 37 °C, 5% CO_2 for 2 h prior to analysis. After incubation, media containing conjugates were discarded. The cells were washed twice with PBS, and then plated onto sterile 35 mm glass bottom dishes with 14 mm microwells (MatTek Corporation, Ashland, MA) for live cell fluorescence imaging using Olympus laser scanning confocal microscope (FV 1000). As controls, cells incubated with FITC-labeled 1F5 mAb, rhodamine-labeled $F(ab')_2$, and PBS were also examined.

2.7. Apoptosis evaluation

Apoptosis induction of Raji cells following exposure to the multivalent conjugates was evaluated by three assays: caspase-3 activation, Annexin V binding, and TUNEL (terminal deoxynucleotide mediated-dUTP nick-end labeling) assay. Quantification of apoptotic activity was performed by flow cytometry, and presented as "apoptotic index" (% apoptotic cells). In all experiments, 1F5 mAb hyper-crosslinked with a goat antimouse (GAM) secondary antibody (2° Ab) (KPL, Gaithersburg, MD) was used as a positive control (molar ratio 1F5:GAM = 3:1). Cells treated with: (a) free anti-CD20 Fab′ fragments, (b) mixture of Fab′ and P-NH_2 (equivalent amounts to conjugates), and (c) culture medium only, were used as negative controls.

2.7.1. Caspase-3 activity—Caspase-3 activity was characterized by analysis of treated cells with the Phi-PhiLux kit (OncoImmunin, Gaithersburg, MD). Prior to analyses, 2.5×10^5 Raji cells were suspended in 0.5 mL fresh growth medium with 2 μM of Fab′ equivalent of conjugates. The cells were treated for 6 h in a humidified atmosphere at 37 °C and 5% CO_2 and then analyzed for caspase-3 activation following the manufacturer's protocol. For treatments using hyper-crosslinked mAb, cells were firstly incubated with 2 μM of 1F5 mAb for 1 h, and then washed twice with PBS + 1% BSA, followed by re-suspension in 0.5 mL of fresh growth medium with 100 μg per mL of GAM. The cells were incubated for another 5 h at 37 °C prior to staining. All experiments were carried out in triplicate.

2.7.2. Annexin V binding—Apoptotic activity was studied by treating Raji cells with conjugates followed by Annexin V staining using the RAPID protocol provided by the manufacturer (Oncogene Research Products, Boston, MA). In addition, Annexin V binding assay was chosen to further study the processes in time- and concentration-dependent manner. For each assay, 2.5×10^5 cells were suspended in 0.5 mL of fresh growth medium with an appropriate amount of conjugate (conjugates in Fab′ equivalent ranged from 1 to 8 μM) and incubated for 20 h, 40 h, or 60 h. For positive controls, cells were treated with 1F5 mAb at concentrations from 1 to 8 μM in growth medium for 1 h. The cells were then washed and suspended in 0.5 mL of fresh growth medium with corresponding amounts of GAM antibody (from 50 to 400 μg per mL) (molar ratio 1F5:GAM = 3:1). The cells were treated for another 19 h, 39 h, or 59 h at 37 °C prior to staining. All experiments were carried out in triplicate.

2.7.3. TUNEL assay—Analysis of DNA fragmentation as characteristics of apoptosis was conducted using the TUNEL assay. In these experiments 7.5×10^5 Raji cells were treated with 2 μM of Fab′ equivalent of conjugates in 0.5 mL of fresh growth medium and allowed to incubate for 20 h. When Raji cells were treated with 2 μM of 1F5 mAb, they were allowed to incubate for 1 h, and then washed twice with PBS + 1% BSA, followed by re-suspension into 0.5 mL of fresh growth media with 100 μg/mL of GAM antibody. The cells were incubated for another 19 h. Prior to analysis, the cells were fixed with 2% paraformaldehyde in PBS for 1 h at room temperature. Cells were then permeabilized in 70% ethanol overnight at 4 °C. Nick-end labeling was done using an Apo Direct TUNEL kit

(Phoenix Flow Systems, San Diego, CA) following the manufacturer's protocol. All experiments were carried out in triplicate.

2.8. Cell viability study

Viabilities of Raji cells after different time of treatments were analyzed by propidium iodide (PI) binding. Quantification of cell viability was performed with flow cytometry. For these experiments, all treatment conditions were identical to those in the time-dependent Annexin V binding assays except for selection of different time intervals for analysis. In brief, cells were incubated with 2 μM (Fab′-equivalent) of HPMA copolymer-Fab′ conjugates (or 1F5 mAb) for 24 h, 48 h, or 72 h (or 1 h for 1F5 mAb followed by exposure to 100 μg/mL of GAM for 23 h, 47 h, and 71 h). All experiments were carried out in triplicate.

2.9. Statistics

All quantified data were presented as mean ± standard deviation (SD). Analyses were performed by the Student's *t* test, with $p < 0.05$ considered as statistically significant.

3. Results & discussion

3.1. Design and synthesis of linear multivalent HPMA copolymer-Fab′ conjugates

Previously, we have demonstrated that attaching multiple Fab′ fragments to soluble, branched HPMA copolymer resulted in antigen binding enhancement [26]. Multivalent HPMA copolymer-Fab′ conjugates showed significant apoptotic activity initiated by crosslinking the B cell antigen CD20 [27]. To further elucidate the relationship between the structure of HPMA copolymer-Fab′ conjugates and their biological activities, a series of linear HPMA copolymers with variable chain lengths and different contents of APMA comonomer (Fab′ attachment points) was designed (Fig. 1 and Table 1). Polymer precursor P1 had the polymer backbone with average molecular weight designed as 100 kDa and contained the lowest amount of pendent amino groups per polymer chain; it served as a "control conjugate". P2 had a doubled backbone length (200 kDa) and identical amino group density with P1. P2a had about a doubled backbone length (200 kDa) but the same amount of pendent amino groups as P1. Comparison of conjugates based on P1, P2, and P2a allowed evaluation of the impacts of both valence and polymer chain length. P2b had the polymer chain length (200 kDa) and pendent group amounts almost identical to P2; however, its backbone contained an enzyme cleavable oligopeptide (GFLG). Comparison of P2b with P2 will permit to evaluate if the insertion of the peptide into polymer backbone would change the flexibility of polymer with impact on biorecognition by CD20 receptors. The degradability of the polymer backbone will be of utmost importance in future *in vivo* study. P3 possessed the longest polymer chain (300 kDa) and the highest amount of amino groups, to assess the impact of multivalency.

As described above, multivalent HPMA copolymer-(anti-CD20) Fab′ conjugates (P-Fab′) were prepared in a three-step process (Fig. 1A). First, the copolymers of HPMA and APMA (P-NH_2) were synthesized by RAFT copolymerization, which permitted to obtain copolymers with precisely designed molecular weight (Mw) and low polydispersity. This process is well controllable; an excellent correlation between theoretical and experimental molecular weights was achieved (Table 1). This is an improvement over the synthesis using traditional radical polymerization [26,27]. Previously, copolymerization of HPMA and APMA was performed in the presence of a small amount of tetraethyleneglycol dimethacrylate and produced branched copolymers with high polydispersity. Consequently, fractionation was required to prepare narrowly dispersed polymer precursors [26].

For the synthesis of biodegradable polymer precursor, a bifunctional chain transfer agent (peptide2CTA) was used. The monomers were incorporated at both dithiobenzoate groups of peptide2CTA with identical efficiency [29] producing a diblock copolymer P2b with an enzyme degradable sequence (GFLG) in the middle of the polymer chain. Such diblock (or multiblock) HPMA polymers have demonstrated excellent backbone degradability in responses to papain and lysosomal enzyme cathepsin B [29,33,34].

After converting pendent amino groups to maleimido groups by reaction with heterobifunctional reagent, SMCC or sulfo-SMCC, HPMA copolymers (P-mal) were conjugated with freshly reduced Fab′ fragments. Representative SEC profiles of P1 and P1-Fab′ are shown in Fig. 2; a significant shift of signal was observed which suggests successful attachment of Fab′ to polymer backbone. Profiles of the other four conjugates are demonstrated in Supplementary Data Fig. S1.

For further characterization of the P-Fab′ conjugates, dynamic light scattering (DLS) was used to determine the hydrodynamic effective diameters of the polymers before and after conjugation with Fab′ (Table 2). To analyze the valence (number of Fab′ fragments per polymer chain), a modified amino acid analysis (AAA) was performed (Table 2 and Fig. S2). The results of DLS on polymer precursors (P-NH_2) and unconjugated Fab′ fragment corresponded well with both published values [35] and our previous observations [26]. For the conjugates, enlargement of the effective diameter was observed. To rule out aggregation, we measured the hydrodynamic volume at different concentrations (Supplementary Data Fig. S3). The increased volume may be explained by dispersive forces between intrachain Fab′ fragments, resulting in the expansion of the polymer coil. In addition, there is a slight possibility of a side reaction between residual amines from P-NH_2 (or amines of Fab′) with the maleimido groups resulting in the formation of interchain covalent crosslinks. Nevertheless, when compared to branched HPMA copolymer-Fab′ conjugates of comparable Mw and valences [26], the effective diameters of linear P-Fab′ are apparently larger. This could have significant impact on *in vivo* circulating half-life and biodistribution.

Several studies have demonstrated the positive correlation between hydrodynamic volumes of HPMA polymers, copolymers, or conjugates and their intravascular half-lives [4,36–38]. Thus, the P-Fab′ conjugates presented here will very likely possess prolonged systematic circulation times. Previous studies on therapeutic mAb or multimeric Ab have pointed out the significant influence of unintended alteration of serum half-life after genetic engineering or physicochemical modification on *in vivo* therapeutic efficacy [22,23,25]. For instance, Popov *et al.* reported the rapid elimination from blood circulation of multivalent rituximab lipid nanoparticles (Ritux-LNPs), and ascribed the observed absence of increase in *in vivo* therapeutic efficacies (when compared to rituximab) to the decreased circulating half-life [23]. The recent design of backbone degradable HPMA copolymers [29,33,34] will permit to use high-Mw, long-circulating conjugates without impairment of therapeutic efficacy.

Confocal fluorescence microscopy (Fig. 3) demonstrated the localization of (rhodamine-labeled) conjugates at the surface of Raji B cell, corresponding to a high expression level of non-internalizing CD20 surface antigen of this cell line. This result further illustrated the successful synthesis of conjugates with retained biological activity of anti-CD20 Fab′ in order to target B cells.

3.2. Relationship between polymer chain length and valence of P-Fab′ conjugates and apoptosis induction in Raji B cells

Previous studies demonstrated that crosslinking of non-internalizing CD20 receptors on Raji B cells results in receptor clustering with concomitant apoptosis induction. The evaluation of apoptosis initiation following Raji B cell exposure to multivalent conjugates was performed

by three distinct assays from differing perspectives: caspase-3 activation (gene expression due to CD20-mediated signaling), Annexin V binding (cell membrane flipping as an early apoptotic event), and the TUNEL assay (DNA fragmentation as a late apoptotic event). Levels of apoptosis induction by the five conjugates (Table 2) were compared; results from the three assays were consistent and showed very similar trends (Fig. 4). P1-Fab′ designed as a "control conjugate" had the weakest apoptotic activity among the five, with only minimal effects detected when compared to the untreated group (culture medium only), unconjugated Fab′, and Fab′+P-NH_2 controls. Conjugate P2-Fab′ with doubled backbone length and doubled valence (than P1-Fab′) produced significant apoptotic levels as expected. Interestingly, P2a-Fab′ with similar valence as P1-Fab′ but a longer polymer chain seemed to have stronger apoptotic efficacy than P1-Fab′ (but less than P2-Fab′), suggesting that in addition to valence, polymer chain length could also be a factor for apoptosis induction. This result is striking because, first, none of the previous literature on multimeric anti-CD20 mAb has published the positive influence of polymer length on apoptosis, and second, Rossi *et al.* suggested the need for clustering at least three CD20 to induce cytotoxicity [25] (noting that the mean valence of P2a-Fab′ is 1.3). Data reported here could be potentially explained by either an improved binding kinetics of the conjugate, or a better range of "reaching" to cluster neighboring CD20 as resulted from the longer polymer chain, although further analysis is necessary.

Furthermore, P2b-Fab′ had almost identical polymer chain length and valence as P2-Fab′ but with a peptide (GFLG)-containing enzyme cleavable backbone. The similar degrees of apoptosis observed in P2b-Fab′ and P2-Fab′ indicate that the insertion of peptide segments into the polymer backbone does not have a noticeable impact on the flexibility of the macromolecule and on its potential to attach to multiple CD20 antigens on the surface of Raji B cells. In addition, these biodegradable HPMA-based polymer carriers [29,33,34] possess favorable properties for *in vivo* applications. They are long-circulating in the bloodstream, their biodegradability profiles can be easily manipulated, they possess favorable pharmacokinetics, and a favorable tumor-to-normal tissue accumulation ratio [4, 39]. Data presented here rationalize the future design of a biodegradable, multiblock P-Fab′ system composed of HPMA copolymer blocks of molecular weight below the renal threshold (40–45 kDa).

The conjugate P3-Fab′ was designed with the longest backbone and highest valence aiming to achieve an optimal biological efficacy. Although the conjugate P3-Fab′ produced the highest apoptotic level among the five conjugates, the enhancement of activity observed at the experimental conditions used (2 μM Fab′-equivalent concentration, 20 h incubation) was modest. We hypothesize that the combination of a high valence (11.3) and a long polymer chain (336 kDa) might result in a solution conformation that renders some Fab′ fragments less accessible (shielded) to interaction with CD20, thus limiting the targeting effect [40]. This explanation was supported by results of DLS (Table 2); P3-Fab′ had a mean hydrodynamic diameter of 97.3 nm–a modest increase when compared to the other conjugates.

3.3. Impact of exposure time and P-Fab′ concentration on apoptosis induction and cytotoxicity

A time-dependent cell viability study (Fig. 5) was performed using propidium iodide (PI) and flow cytometry. PI is a fluorescent DNA-intercalating agent commonly used to bind and detect nonviable cells, or to distinguish late apoptotic cells depending on the experimental setup [41]; here we applied the former to stain and quantify all nonviable cells. The viability of Raji cells was analyzed at varying time intervals after exposure to multivalent conjugates at similar conditions as used in apoptosis assays described above. The cytotoxicity of conjugates demonstrated a slower onset at shorter exposure times (24 h, 48 h) than the

whole 1F5 mAb hyper-crosslinked with a secondary Ab (mAb+2°Ab); however, at the longer time interval (72 h) the conjugates appeared to be more effective. For instance, at 72 h, conjugates P2-Fab′ and P2b-Fab′ showed comparable effects as the positive control (mAb+2°Ab), while P3-Fab′ achieved a significantly better efficacy. In the time-dependent apoptosis evaluation (Fig. 6A) using Annexin V assay, the onset patterns of apoptosis were the same as observed in the cytotoxicity assay. Both P2-Fab′ and P3-Fab′ reached comparable levels of early apoptosis as the positive control at longer exposure times (40 h, 60 h). In particular, at 60 h, the apoptotic activity of P3-Fab′ exceeded that of the positive control ($p < 0.05$). Since the trends of cytotoxicity compared well with results of apoptosis, we speculate that the PI-positive cells primarily resulted from CD20 clustering (late apoptotic cells); however, the potential contribution of cell necrosis cannot be ruled out. These data and the previous observation that the therapeutic efficacy of anti-CD20 mAb may result in direct eradication of B lymphomas [10,11,18] bode well for the potential of P-Fab′ conjugates as therapeutics for NHL.

The concentration (dose)-dependent apoptosis assay (Fig. 6B) revealed an increase of apoptotic index with increasing concentration for all compounds tested. However, the dose-escalation effect was stronger in the positive control group (mAb+2°Ab) than in multivalent conjugates P2-Fab′ and P3-Fab′. In addition, within the concentration range used (1–8 μM), saturation of apoptotic index at high concentrations was not observed in contrast to results obtained with branched polymer-Fab′ conjugates [27]. This suggests a better accessibility of Fab′ fragments bound to linear polymer chains when compared to branched conjugates. This hypothesis is further supported by the comparison of effective diameters of conjugates; the linear P-Fab′ conjugates possess larger hydrodynamic sizes than branched conjugates with equivalent Mw, polydispersity, and valency.

The data seem to suggest that to achieve enhanced biological activities, a long exposure time of linear P-Fab′ was more important than a high Fab′-equivalent concentration. Two factors may contribute to this phenomenon: (a) shielding effect [40], and (b) different binding kinetics to CD20 between P-Fab′ and mAb followed by 2°Ab. The impact of time corresponds well with the design of backbone degradable, long-circulating conjugates. Optimization of the structure of conjugates based on the best combination of molecular weight and valency needs to be undertaken.

4. Conclusions

A hybrid biomimetic system composed of RAFT-synthesized, linear, high-Mw HPMA copolymers grafted with multiple anti-CD20 Fab′ fragments was designed. The preparation methods did not require fractionation by SEC, thus are well suited for scale-up. The technique enabled synthesis of conjugates with low poly-dispersity and tailor-made properties to study the structure-activity relationship. The biorecognition of multivalent P-Fab′ conjugates by CD20 receptors on the surface of Raji B cells was visualized by confocal fluorescence microscopy. Crosslinking of CD20 receptors on the surface of Raji B cells induced apoptosis as determined by caspase-3 activity, Annexin V binding, and TUNEL assays. Both polymer chain length and valence (amount of Fab′ per chain) were factors having an impact on apoptotic efficiency, whereas insertion of a peptide into the HPMA copolymer backbone was not. In addition, long exposure time of the conjugates with Raji B cells resulted in enhanced apoptosis and higher cytotoxicity when compared to whole anti-CD20 mAb hyper-crosslinked by a secondary Ab; high dose (concentration) seemed to be less influential. The present system possesses ideal architecture (linear) and characteristics (suitable hydrodynamic size, as analyzed by DLS) to allow the further design of long-circulating biodegradable systems. Based on the presented data and the favorable characteristics of CD20 (non-internalizing, not present in serum under standard conditions,

with no known natural ligand) as a target for B lymphoma, this study provides a potential strategy for the improved treatment of NHL and other B malignancies through direct induction of apoptosis without Fc-related mechanisms and side effects.

Supplementary Material

Refer to Web version on PubMed Central for supplementary material.

Acknowledgments

The research was supported in part by NIH grant GM95606 from the National Institute of General Medical Sciences and the University of Utah Research Foundation. We thank Dr. Pavla Kopečková for helpful discussion.

References

1. Couvreur P, Vauthier C. Nanotechnology: intelligent design to treat complex disease. Pharm Res. 2006; 23(7):1417–50. [PubMed: 16779701]
2. Kopeček J. Smart and genetically engineered biomaterials and drug delivery systems. Eur J Pharm Sci. 2003; 20(1):1–16. [PubMed: 13678788]
3. Kopečcek J, Kopečková P. HPMA copolymers: origins, early developments, present, and future. Adv Drug Deliv Rev. 2010; 62(2):122–49. [PubMed: 19919846]
4. Ulbrich K, Šubr V. Structural and chemical aspects of HPMA copolymers as drug carriers. Adv Drug Deliv Rev. 2010; 62(2):150–66. [PubMed: 19931329]
5. Vicent MJ, Ringsdorf H, Duncan R. Polymer therapeutics: clinical applications and challenges for development. Adv Drug Deliv Rev. 2009; 61(13):1117–20. [PubMed: 19682516]
6. Wu K, Liu J, Johnson RN, Yang J, Kopeček J. Drug-free macromolecular therapeutics: induction of apoptosis by coiled-coil-mediated cross-linking of antigens on the cell surface. Angew Chem Int Ed Engl. 2010; 49(8):1451–5. [PubMed: 20101660]
7. Wu K, Yang J, Liu J, Kopeček J. Coiled-coil based drug-free macromolecular therapeutics: in vivo efficacy. J Control Release. 2012; 157(1):126–31. [PubMed: 21843563]
8. Siegel R, Naishadham D, Jemal A. Cancer statistics. CA Cancer J Clin. 2012; 62(1):10–29. [PubMed: 22237781]
9. Stashenko P, Nadler LM, Hardy R, Schlossman SF. Characterization of a human B lymphocyte-specific antigen. J Immunol. 1980; 125(4):1678–85. [PubMed: 6157744]
10. Cheson BD, Leonard JP. Monoclonal antibody therapy for B-cell non-Hodgkin's lymphoma. N Engl J Med. 2008; 359(6):613–26. [PubMed: 18687642]
11. Molina A. A decade of rituximab: improving survival outcomes in non-Hodgkin's lymphoma. Annu Rev Med. 2008; 59:237–50. [PubMed: 18186705]
12. Allison M. PML problems loom for rituxan. Nat Biotechnol. 28(2):105–6. [PubMed: 20139927]
13. Major EO. Reemergence of PML in natalizumab-treated patients–new cases, same concerns. N Engl J Med. 2009; 361(11):1041–3. [PubMed: 19741226]
14. Lands LC. New therapies, new concerns: rituximab-associated lung injury. Pediatr Nephrol. 2010; 25(6):1001–3. [PubMed: 20195643]
15. Kamei K, Ito S, Iijima K. Severe respiratory adverse events associated with rituximab infusion. Pediatr Nephrol. 2010; 25(6):1193. [PubMed: 20024586]
16. Cartron G, Dacheux L, Salles G, Solal-Celigny P, Bardos P, Colombat P, et al. Therapeutic activity of humanized anti-CD20 monoclonal antibody and polymorphism in IgG Fc receptor FcgRIIIa gene. Blood. 2002; 99(3):754–8. [PubMed: 11806974]
17. van der Kolk LE, Grillo-López AJ, Baars JW, Hack CE, van Oers MH. Complement activation plays a key role in the side effects of rituximab treatment. Br J Haematol. 2001; 115(4):807–11. [PubMed: 11843813]
18. Smith MR. Rituximab (monoclonal anti-CD20 antibody): mechanisms of action and resistance. Oncogene. 2003; 22(47):7359–68. [PubMed: 14576843]

19. de Haij S, Jansen JHM, Boross P, Beurskens FJ, Bakema JE, Bos DL, et al. In vivo cytotoxicity of type I CD20 antibodies critically depends on Fc receptor ITAM signaling. Cancer Res. 2010; 70(8):3209–17. [PubMed: 20354182]
20. Golay J, Cittera E, Di Gaetano N, Manganini M, Mosca M, Nebuloni M, et al. The role of complement in the therapeutic activity of rituximab in a murine B lymphoma model homing in lymph nodes. Haematologica. 2006; 91(2):176–83. [PubMed: 16461301]
21. Stein R, Qu Z, Chen S, Solis D, Hansen HJ, Goldenberg DM. Characterization of a humanized IgG4 anti-HLA-DR monoclonal antibody that lacks effector cell functions but retains direct antilymphoma activity and increases the potency of rituximab. Blood. 2006; 108(8):2736–44. [PubMed: 16778139]
22. Zhang N, Khawli LA, Hu P, Epstein AL. Generation of rituximab polymer may cause hyper-cross-linking–induced apoptosis in non-Hodgkin's lymphomas. Clin Cancer Res. 2005; 11(16):5971–80. [PubMed: 16115941]
23. Popov J, Kapanen AI, Turner C, Ng R, Tucker C, Chiu G, et al. Multivalent rituximab lipid nanoparticles as improved lymphoma therapies: indirect mechanisms of action and in vivo activity. Nanomedicine (Lond). 2011; 6(9):1575–91. [PubMed: 22011314]
24. Ghetie MA, Bright H, Vitetta ES. Homodimers but not monomers of rituxan (chimeric anti-CD20) induce apoptosis in human B-lymphoma cells and synergize with a chemotherapeutic agent and an immunotoxin. Blood. 2001; 97(5):1392–8. [PubMed: 11222385]
25. Rossi EA, Goldenberg DM, Cardillo TM, Stein R, Wang Y, Chang C-H. Novel designs of multivalent anti-CD20 humanized antibodies as improved lymphoma therapeutics. Cancer Res. 2008; 68(20):8384–92. [PubMed: 18922911]
26. Johnson RN, Kopečková P, Kopeček J. Synthesis and evaluation of multivalent branched HPMA copolymer–Fab′ conjugates targeted to the B-cell antigen CD20. Bioconjug Chem. 2009; 20(1): 129–37. [PubMed: 19154157]
27. Johnson RN, Kopečková P, Kopeček J. Biological activity of anti-CD20 multivalent HPMA copolymer-Fab′ conjugates. Biomacromolecules. 2012; 13(3):727–35. [PubMed: 22288884]
28. Kopeček J, Bažilová H. Poly[*N*-(2-hydroxypropyl)methacrylamide]. I. Radical polymerization and copolymerization. Eur Polym J. 1973; 9(1):7–14.
29. Pan H, Yang J, Kopečková P, Kopeček J. Backbone degradable multiblock *N*-(2-hydroxypropyl)methacrylamide copolymer conjugates via reversible addition-fragmentation chain transfer polymerization and thiolene coupling reaction. Biomacromolecules. 2011; 12(1):247–52. [PubMed: 21158387]
30. Starcher B. A ninhydrin-based assay to quantitate the total protein content of tissue samples. Anal Biochem. 2001; 292(1):125–9. [PubMed: 11319826]
31. Ellman GL. Tissue sulfhydryl groups. Arch Biochem Biophys. 1959; 82(1):70–7. [PubMed: 13650640]
32. Omelyanenko V, Kopečková P, Gentry C, Shiah JG, Kopeček J. HPMA copolymer-anticancer drug-OV-TL16 antibody conjugates. 1. Influence of the method of synthesis on the binding affinity to OVCAR-3 ovarian carcinoma cells in vitro. J Drug Target. 1996; 3(5):357–73. [PubMed: 8866655]
33. Luo K, Yang J, Kopečková P, Kopeček J. Biodegradable multiblock poly[*N*-(2-hydroxypropyl)methacrylamide] via reversible addition–fragmentation chain transfer polymerization and click chemistry. Macromolecules. 2011; 44(8):2481–8. [PubMed: 21552355]
34. Yang J, Luo K, Pan H, Kopečková P, Kopeček J. Synthesis of biodegradable multiblock copolymers by click coupling of RAFT-generated heterotelechelic polyHPMA conjugates. React Funct Polym. 2011; 71(3):294–302. [PubMed: 21499527]
35. Allen TM, Brandeis E, Hansen CB, Kao GY, Zalipsky S. A new strategy for attachment of antibodies to sterically stabilized liposomes resulting in efficient targeting to cancer cells. Biochim Biophys Acta. 1995; 1237(2):99–108. [PubMed: 7632714]
36. Lammers T, Kühnlein R, Kissel M, Šubr V, Etrych T, Pola R, et al. Effect of physicochemical modification on the biodistribution and tumor accumulation of HPMA copolymers. J Control Release. 2005; 110(1):103–18. [PubMed: 16274831]

37. Shiah J-G, Dvořák M, Kopečková P, Sun Y, Peterson CM, Kopeček J. Bio-distribution and antitumour efficacy of long-circulating *N*-(2-hydroxypropyl) methacrylamide copolymer-doxorubicin conjugates in nude mice. Eur J Cancer. 2001; 37(1):131–9. [PubMed: 11165140]

38. Allmeroth M, Moderegger D, Biesalski B, Koynov K, Rosch F, Thews O, et al. Modifying the body distribution of HPMA-based copolymers by molecular weight and aggregate formation. Biomacromolecules. 2011; 12(7):2841–9. [PubMed: 21692523]

39. Kopecek, J.; Kopečková, P. Design of polymer-drug conjugates. In: Kratz, F.; Senter, P.; Steinhagen, H., editors. Drug delivery in oncology. Vol. 2. Weinheim: Wiley-VCH; 2012. p. 485-512.

40. Ding H, Kopečková P, Kopeček J. Self-association properties of HPMA copolymers containing an amphipathic heptapeptide. J Drug Target. 2007; 15(7–8):465–74. [PubMed: 17671893]

41. Hervé L. Nuclear apoptosis detection by flow cytometry: influence of endogenous endonucleases. Exp Cell Res. 2002; 277(1):1–14. [PubMed: 12061813]

Appendix A. Supplementary material

Supplementary material associated with this article can be found, in the online version, at doi:10.1016/j.biomaterials.2012. 06.024.

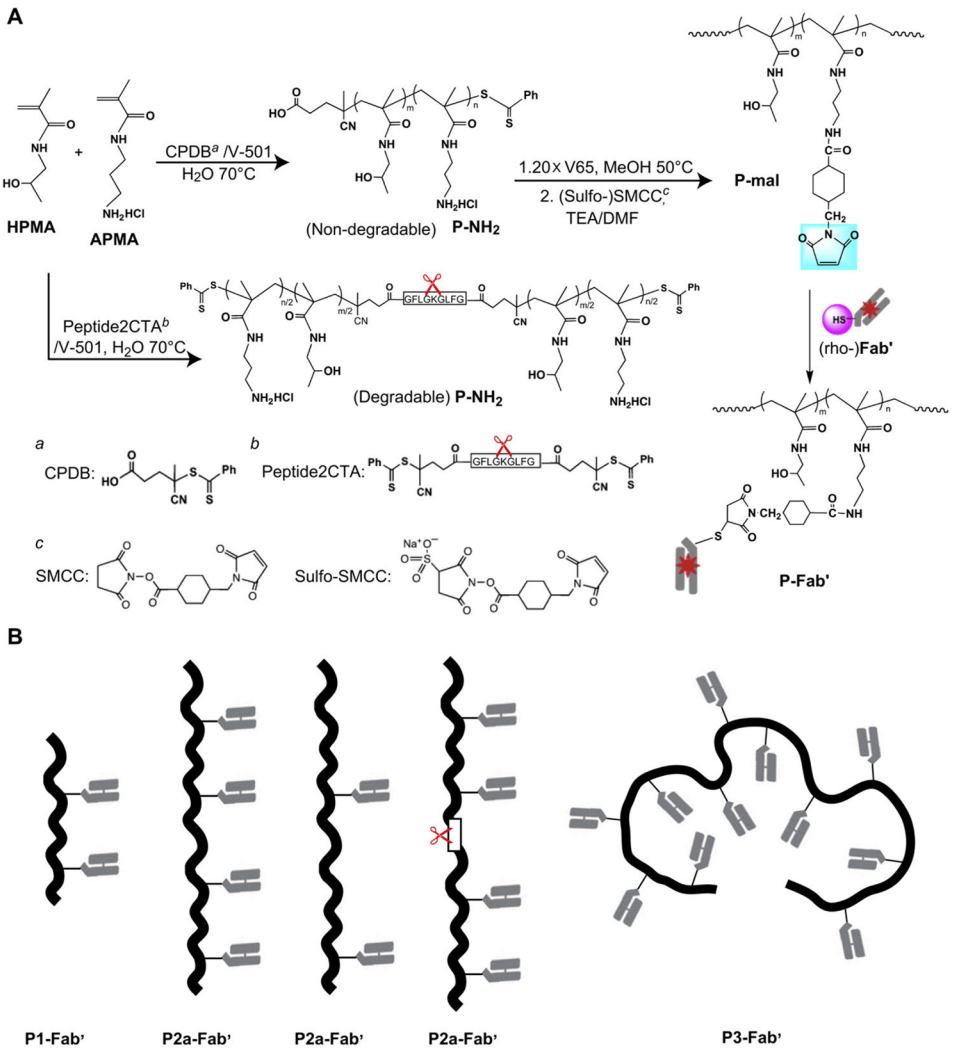

Fig. 1.

Synthesis of multivalent HPMA copolymer-Fab′ conjugates targeted to B cell antigen CD20. (A) Schemes for the synthesis of polymer precursors (P-NH_2, P-mal) and multivalent conjugates (P-Fab′). (B) Schematics of polymer conjugate architectures.

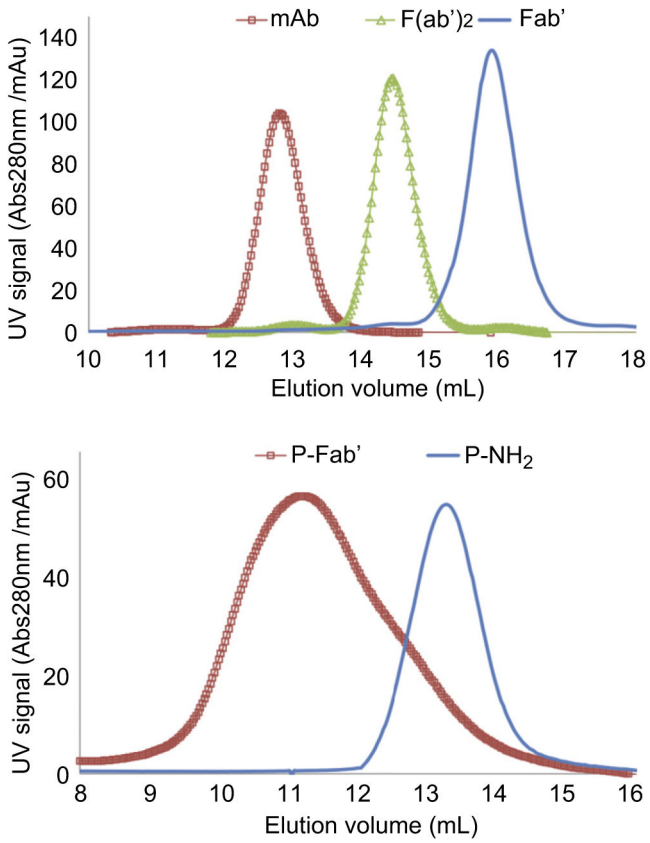

Fig. 2.

(Top panel) SEC profiles of harvested 1F5 mAb, digested F(ab′)$_2$ and reduced Fab′ fragments by ÄKTA FPLC (Superdex 200 HR10/30 column, PBS). Purity of all products from each step were >95%. **(Bottom panel)** SEC profiles of representative P-NH$_2$ (P1) and P-Fab′ (P1-Fab′) by ÄKTA FPLC (Superpose 6 HR10/30 column, acetate buffer + 30% acetonitrile v/v).

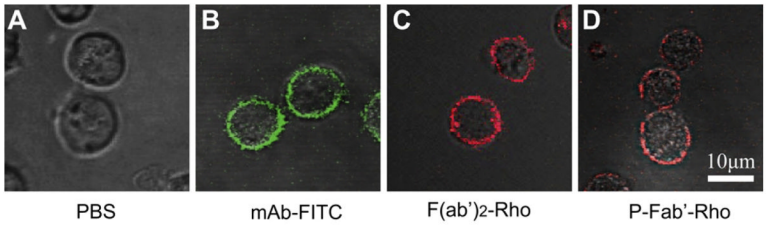

Fig. 3.

Confocal fluorescence microscopic images of Raji B cells exposed to (A) PBS, (B) 1F5 mAb labeled with FITC, (C) $F(ab')_2$ antibody fragment labeled with rhodamine, and (D) P-Fab′ conjugate labeled with rhodamine. Raji cells (2.5×10^5) were stained with varying concentrations of each compound for 2 h prior to analysis.

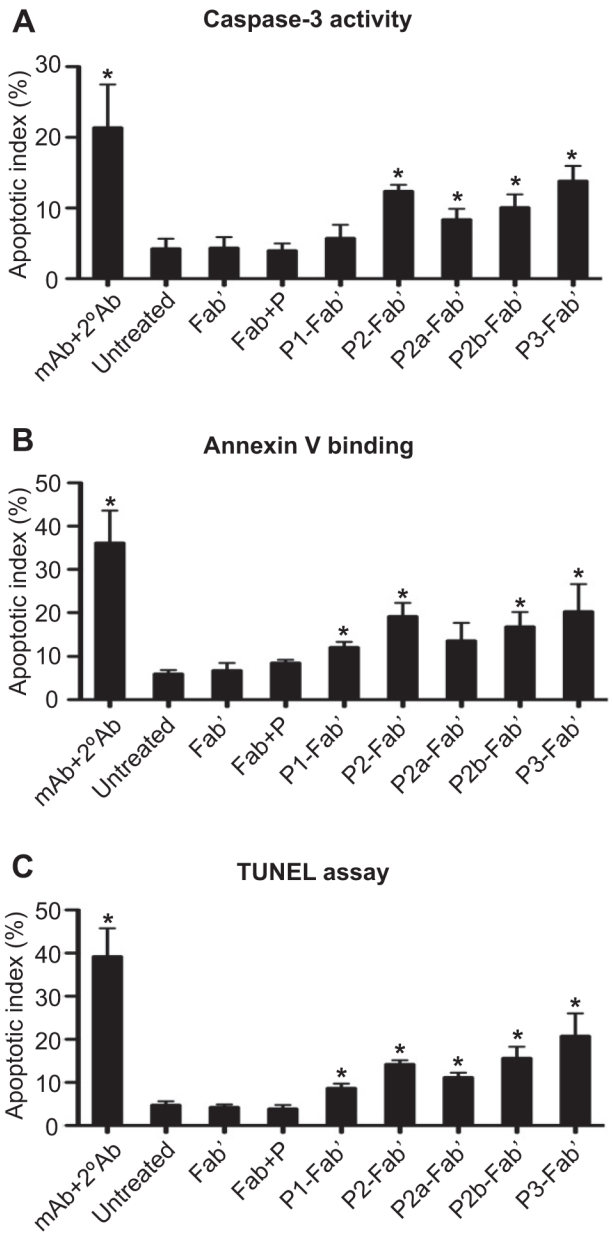

Fig. 4.

Apoptosis induction of Raji B cell analyzed by (A) caspase-3 activity, (B) Annexin V binding, and (C) TUNEL assays. Quantification was performed by flow cytometry. All experiments were carried out in at least triplicate (data shown as mean ± SD). Statistics was performed by comparing each group with the untreated (*: $p < 0.05$).

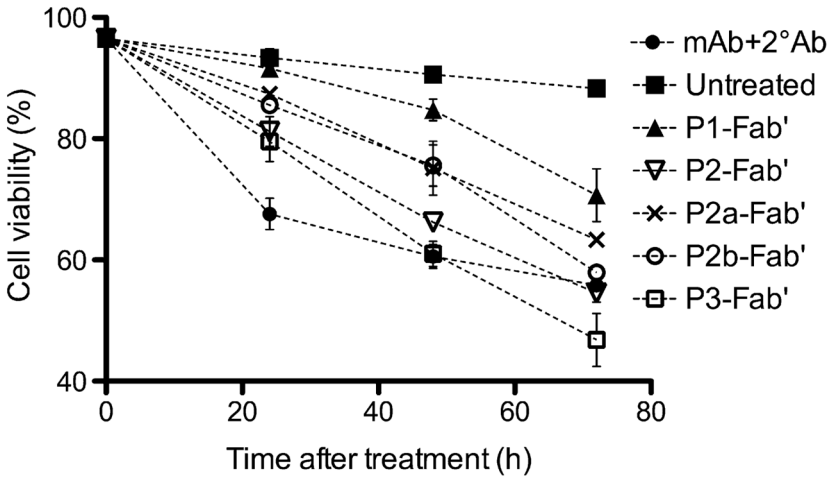

Fig. 5.

Time-dependent cell viability study assessed by propidium iodide (PI) binding. Treatment conditions were identical to apoptosis assays. Quantification was performed by flow cytometry. Experiments were carried out in triplicate (data shown as mean ± SD). (■) Untreated; (●) mAb+2°Ab; (▲) P1-Fab′; (▽) P2-Fab′; (×) P2a-Fab′; (○) P2b-Fab′; (□) P3-Fab′.

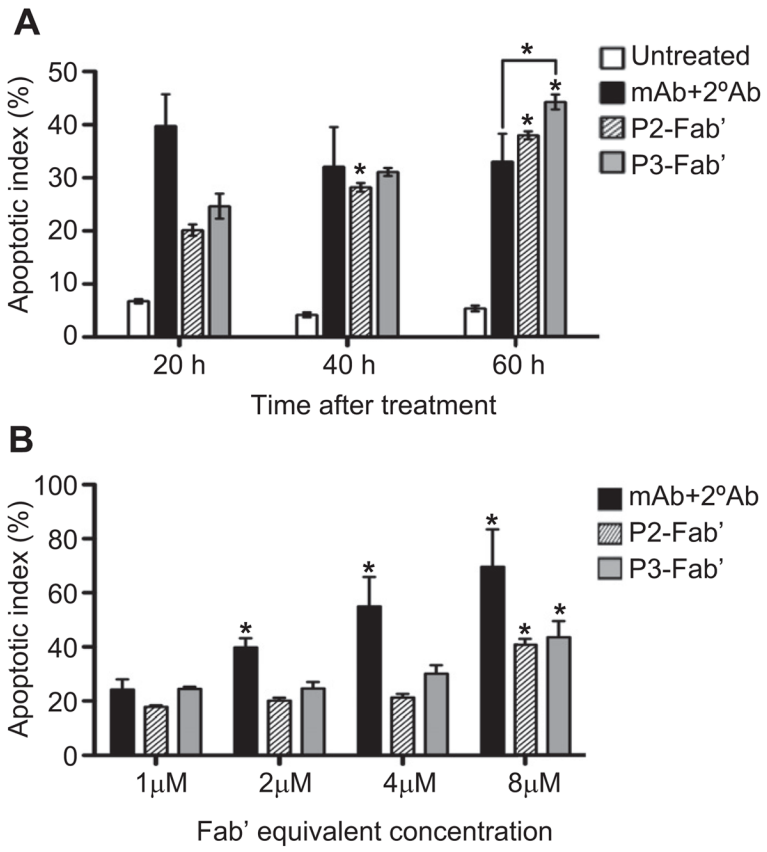

Fig. 6.

Cell apoptosis evaluated by Annexin V binding in (A) time-dependent, and (B) concentration-dependent assays. All experiments were carried out in triplicate (data shown as mean ± SD). Statistical analyses (unless otherwise indicated) were performed by comparing each group with the corresponding shortest time interval or lowest concentration (*: $p < 0.05$, by Student's *t* test).

Table 1

Synthesis and characterization of P-NH_2 polymer precursors.

No.	$[M]_0$:$[CTA]_0$:$[I]_0$	Conv.[a] %	M_w (kDa)			NH_2 mol.%		
			Theo.[b]	SEC[c]	M_w/M_n	In feed	Found[d]	Structure
P1	800:1:0.33	87.3	102	105	1.09	6	4.31	Non-degradable
P2	1600:1:0.33	89.4	208	207	1.07	6	4.13	Non-degradable
P2a	1600:1:0.33	94.9	219	223	1.04	3	2.12	Non-degradable
P2b[e]	1600:1:0.25	84.1	197	201	1.11	6	4.23	Degradable
P3	3000:1:0.33	75.7	330	336	1.05	6	4.75	Non-degradable

[a] Conversion estimated by weight % polymer products.

[b] Theoretical molecular weight of polymer calculated by the following equation: $M_{w\text{theo.}}$ = [([M]0 ÷ [CTA]0) × Conversion × Mean M_w of monomers] + M_w of CTA.

[c] Average molecular weight and polydispersity determined by SEC.

[d] Amine content (NH_2 mol.%) determined by ninhydrin assay.

[e] Modified CPDB containing enzyme cleavable peptide was used as chain transfer agent (CTA).

Biomaterials. Author manuscript; available in PMC 2013 October 01.

Table 2

Characterization of P-Fab′ conjugates.

No.	Valence[a]	Effective diameter[b] (nm)	
		before conj.	after conj.
P1-Fab′	1.7	12.4	36.2
P2-Fab′	3.3	19.1	82.3
P2a-Fab′	1.3	21.1	56.3
P2b-Fab′[c]	3.4	21.6	74.3
P3-Fab′	11.3	27.4	97.3
Fab′	–	4.5	–
P-3Fab3.2[d]	3.2	–	30.2

[a] Fab′ per polymer chain as determined by modified AAA.

[b] Determined by DLS (all samples with polydispersity <0.2).

[c] Degradable backbone containing GFLG oligopeptide.

[d] Branched conjugates with polymer M_W = 193 kDa [26].